107

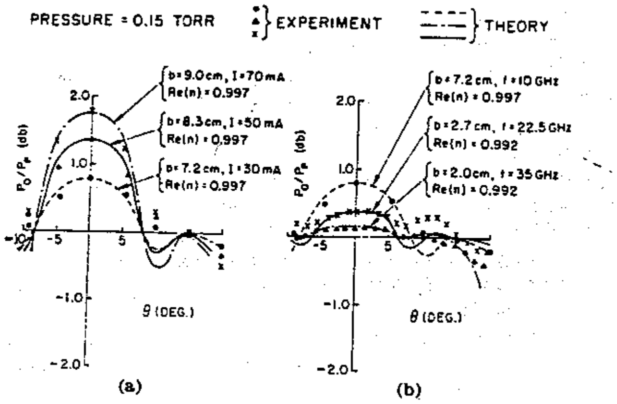

Fig. 1. Power changes as a function of scattering angle. (a) Constant frequency and changing discharge current; $f = 10$ GHz. (b) Constant discharge current and various frequencies; $I = 30$ mA.

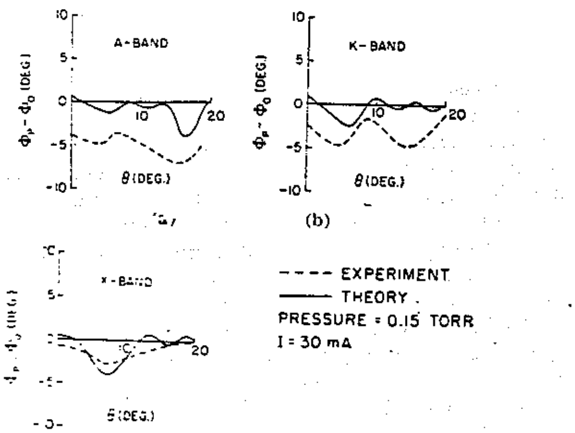

Fig. 2. Phase changes as a function of scattering angle for constant discharge current. (a) $f = 35$ GHz. (b) $f = 22.5$ GHz. (c) $f = 10$ GHz.

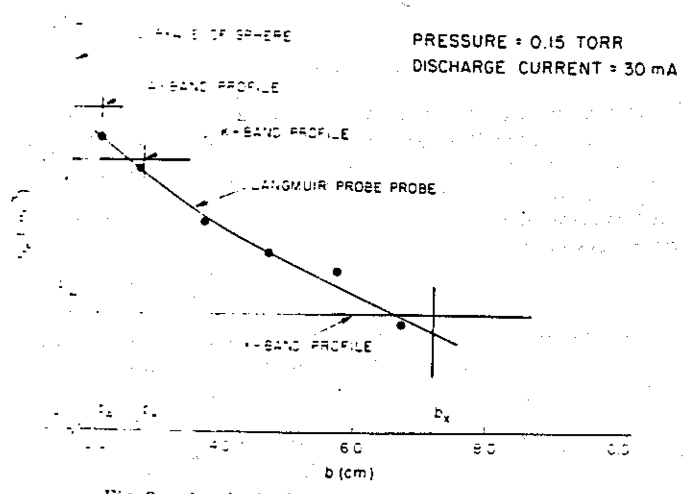

Fig. 3. Synthesized electron density distribution.

of the plasma frequency to incident wave frequency.) A synthesized N_e profile for the plasma-conductor configuration under discussion is shown in Fig. 3 along with the profile determined by Langmuir probe measurements.

For the present laboratory conditions and the model chosen, the calculated values of P_0/P_p and $\Phi_p - \Phi_0$ change slowly as functions of n and b. As a consequence, the n and b that one can choose to match theory and experiment equally well can only be determined within a range of values. In Fig. 3, the crosses at the beginning of each rectangular profile indicate these ranges. To determine $N_e(r)$ more closely, a more sophisticated model, such as representing the plasma by many layers, must be used.

T. G. Twardeck[1]
Robert G. Quinn
Ionosphere Research Lab.
Dept. of Elec. Engrg
Pennsylvania State University
University Park, Pa.

References

[1] M. A. Heald and C. B. Wharton, *Plasma Diagnostics with Microwaves*. New York: Wiley, 1965, ch. 7.
[2] R. H. Huddlestone and S. L. Leonard, *Plasma Diagnostic Techniques*. New York: Academic Press, 1965, ch. 11.
[3] W. B. Baker, M. P. Bachynski, and A. I. Carswell, "Electromagnetic wave scattering by plasma coated re-entry bodies," RCA Victor Co., Ltd., Montreal, Canada, Res. Rept. TM7-801-012, November 1964.
[4] P. E. Bisbing, "Electromagnetic scattering by an exponentially inhomogeneous plasma sphere," *IEEE Trans. Antennas and Propagation*, vol. AP-14, pp. 219–224, March 1966.
[5] R. L. Easley, "Diagnosis of plasma cylinders by angular scattering of microwaves," U. S. Army Miccles Command, Redstone Arsenal, Ala., Rept. RR-TR-63-14, May 1963.
[6] V. A. Erma, "Radar cross sections of inhomogeneous plasma spheres, part I," Astrophysics Res. Corp., Los Angeles, Calif., April 1965.
[7] A. R. Jones and E. R. Wooding, "Angular distribution of radiation scattered coherently by a plasma cylinder," *J. Appl. Phys.*, vol. 37, pp. 4670–4676, December 1966.
[8] E. R. Nagelberg, "Microwave interaction with bounded gyro-electric plasmas," Antenna Lab., California Institute of Technology, Pasadena, Tech. Rept. 31, April 1964.
[9] R. G. Quinn and C. C. Chang, "Experimental observations of a stable plasma belt trapped in a dipolar magnetic field," *J. Geophys. Res.*, vol. 71, p. 253, 1966.

[1] Now with NASA/Electronics Research Center, Cambridge, Mass 02139.

On VLF Radiation Fields Along the Static Magnetic Field from Sources Immersed in a Magnetoplasma

***Abstract*—The focusing of waves from radiating VLF sources immersed in a cold magnetoplasma is investigated for the case in which the focusing takes place along the static magnetic field direction. The explicit form of tensor Green's function valid along the field line is derived for the far field, and the frequency ranges where focusing may be expected are specified. The theory is applied to calculate the power flux along the field line for an electric dipole and a magnetic loop with two orientations with respect to the static magnetic field.**

I. Introduction

It has been suggested [1] that important knowledge regarding the origin and nature of VLF emissions could be obtained by the controlled stimulation of these emissions using a VLF transmitter aboard a magnetospheric satellite. Although in theory this stimulation can be accomplished in a number of ways, the possibility of stimulating VLF emissions with man-made signals has actually been proved only for waves which propagate approximately parallel to the earth's magnetic field [2]. Thus it can be anticipated that an important mode of operation for the VLF satellite transmitting system will be one in which the production of longitudinally propagating waves is optimized. The difficulty of the problem of optimization is compounded by the fact that, in general, the stimulation of emissions would be effected at transmitter frequencies below the local electron gyrofrequency (in the range 2 to 20 kHz) where the radiation efficiency of practically sized antenna arrays will be quite low.

Since the output power of the satellite transmitter will be limited by payload restrictions, low values of antenna radiation efficiency can be equated with low values of radiated power. In this case, the possibility of generating longitudinally propagating waves of sufficient amplitude to stimulate VLF emissions could well depend upon the existence of focusing effects in the medium which would

Manuscript received April 24, 1969. This research was supported by NASA under Grant NsG 174-SC/05-020-008.

serve to increase the relative field strength of waves propagating parallel to the field lines. Thus the consideration of focusing effects along the magnetic field lines would appear to be of significant importance in the design of any VLF satellite transmitting system.

Insight into the problem of the focusing of radiation from sources in the magnetosphere can be obtained by considering the idealized case of radiation from sources in a cold, uniform magnetoplasma. The asymptotic evaluation of the far fields produced by sources in such a medium has been made by a number of workers, and focusing effects have been discussed [3]–[6]. However, for observation points located along the static magnetic field lines which intersect the source, the asymptotic calculations of the far fields reported in these papers need to be modified. In this communication, we shall investigate the far fields along the field line in detail by calculating the explicit forms of the tensor Green's function valid along the intersecting field lines for frequencies approximately within the VLF range, that is, between the proton and electron gyrofrequency. Application of the theory is then made by calculating the ray functions along the field line from several elementary sources, and a brief discussion of VLF focusing effects is given.

II. Basic Formulation and Analysis

In a linear, uniform cold magnetoplasma, the electric field excited by a monochromatic ($\exp j\omega t$) current source $J(r)$ can be expressed by the relation

$$E(r) = \int \hat{G}(r - r') \cdot J(r')\, dr'. \tag{1}$$

The tensor Green's function $\hat{G}$ is defined by

$$\hat{G}(r - r') = \hat{D} I(r - r') \tag{2}$$

where

$$\hat{D} = \omega\mu_0 (2\pi k_0)^{-2} (\nabla\nabla\nabla^2 + k_0^2 \hat{L} + k_0^4 \hat{E}) \tag{3}$$

$$I(r - r') = j(2\pi k_0)^{-1} \cdot \int_{-\infty}^{\infty} \int_0^{\pi/2} \int_0^{2\pi} \frac{n^2 \sin\theta \exp - jk_0(r - r')\cdot n}{\alpha(\theta)[n^2 - n_1^2(\theta)][n^2 - n_2^2(\theta)]}\, d\psi\, d\theta\, dn$$

where $r = |r|$, $n = |k/k_0|$, θ is the polar angle between k (wave vector) and the static magnetic field (oriented along positive z axis), ψ is the azimuthal angle of n about the static magnetic field, and

$$n_{1,2}^2(\theta) = \frac{(\epsilon_{+1}\epsilon_{-1} - \epsilon_0\epsilon_s)\sin^2\theta + 2\epsilon_0\epsilon_s \pm q(\theta)}{2\alpha(\theta)}$$

$$q(\theta) = [(\epsilon_0\epsilon_s - \epsilon_{+1}\epsilon_{-1})\ \sin^4\theta + 4\epsilon_0^2\epsilon_d^2 \cos^2\theta]^{1/2}$$

$$\alpha(\theta) = \epsilon_s \sin^2\theta + \epsilon_0 \cos^2\theta$$

$$\epsilon_s = (\epsilon_{+1} + \epsilon_{-1})/2, \quad \epsilon_d = (\epsilon_{-1} - \epsilon_{+1})/2,$$

$$\epsilon_\nu = 1 - \sum_s [X_s/(1 + \nu Y_s)].$$

In the last relation above, X and Y are standard notations for the normalized frequencies in the magnetoionic theory, see, e.g., Ratcliffe [7] and the sum is taken over all particle species with $\nu = +1, -1, 0$.

In terms of the Cartesian components of the relative permittivity tensor, the explicit forms of the tensors $\hat{L}$ and $\hat{E}$ have been developed by Kogelnik [6]. In terms of the principal components of the relative permittivity tensor, L and E can be expressed in the form:

where $\nabla_\perp^2 = \nabla^2 - (\partial^2/\partial z^2)$. For wave frequencies between the proton and electron gyrofrequencies in a plasma modeled upon the magnetosphere, it can be shown from (3) that the square of the refractive index of the ordinary mode $n_1^2(\theta) < 0$ for all θ, and thus this mode is always nonpropagating. On the other hand, for the whistler (or extraordinary) mode, $n_2^2(\theta) > 0$ for all θ when $\omega \le \omega_{LHR}$ (ω_{LHR} = the angular frequency of lower hybrid resonance); when $\omega > \omega_{LHR}$, $n_2^2(\theta) > 0$ for $0 \le \theta \le \theta_r$ ($\theta_r = \arctan(-\epsilon_0/\epsilon_s)^{1/2}$) and $n_2^2(\theta) < 0$ for $\theta_r < \theta < \pi/2$. Since the fields due to the nonpropagating modes decay exponentially away from the source, only the poles from $n_2^2(\theta)$ within the propagating range of θ contribute to the radiation field.

Selecting the pole of $n_2^2(\theta)$ corresponding to outgoing waves, the contour integration with respect to the variable n and the integration with respect to azimuthal angle ψ can be performed in $I(R)$ to yield

$$I(R) = -2\pi k_0^{-1} \int_0^{\pi/2, \theta_r} q^{-1}(\theta) n_2 \sin\theta J_0(k_0\mu(\theta)\tilde{\rho}) \cdot \exp(-jk_0 v(\theta)\, |\tilde{z}|)\, d\theta \tag{5}$$

where $R = r - r'$, $\tilde{\rho}$ and $\tilde{z}$ are the respective transverse and longitudinal components of R in cylindrical coordinates, $v(\theta) = n_2(\theta)\cos\theta$, $\mu(\theta) = n_2(\theta)\sin\theta$, and J_0 is the zero order Bessel function of first kind. The upper limits $\pi/2$ and θ_r apply for the cases $\omega \le \omega_{LHR}$ and $\omega > \omega_{LHR}$, respectively. By the use of large argument approximation of J_0, the asymptotic evaluation of $I(R)$, for $R \to \infty$, has been considered by a number of previous workers [3]–[6]. However, their method is not necessarily correct if it is wished to evaluate the far field along the direction of the static magnetic field lines (the z axis), since the source dimensions may be such that the argument of the Bessel function is not large at the saddle point [8]. This would prove to be the general case; for instance, for VLF sources in the magnetosphere assuming the dimensions of these sources were of the order 10^3 m or less [9].

In these cases where $k_0\mu(\theta)\tilde{\rho} < 1$ at the saddle point, the large argument approximation of J_0 should not be used but instead, for a fixed $\tilde{\rho}$ and $|\tilde{z}| \to \infty$, $I(R)$ can be estimated by the method of stationary phase with the mth-order stationary point defined by

$$(\partial^i/\partial\theta^i) v(\theta) = 0, \quad i = 1, \cdots, m;$$

$$(\partial^{m+1}/\partial\theta^{m+1}) v(\theta) \ne 0. \tag{6}$$

The amount of algebra involved in the asymptotic evaluation of $I(R)$ can be considerably reduced if it is assumed that the electron plasma frequency is large compared to the electron gyrofrequency (i.e., $\omega_{0e}^2 \gg \omega_{He}^2$), a condition which holds throughout the inner magnetosphere ($L \le 4$). In this case, the leading terms in $I(R)$ are given by one of the following three expressions.

Case A

For wave frequencies in either of the two ranges $\omega_{He} > \omega > \frac{1}{2}\omega_{He}$ or $\omega_{LHR} > \omega > \omega_{Hp}$ (ω_{Hp} = proton gyrofrequency), there exists a single stationary point at $\theta = 0$, and $I(R)$ has the form

$$I_A(\tilde{z}) \cong \frac{-2\pi j\lambda \exp(-jk_0\sqrt{\epsilon_{+1}}\, |\tilde{z}|)}{k_0^2\epsilon_0\epsilon_s(1 + \lambda)(1 + 2\lambda)\, |\tilde{z}|}, \quad \lambda = \frac{\epsilon_s}{\epsilon_d}. \tag{7}$$

$$\hat{L} = \begin{bmatrix} \epsilon_s\nabla_\perp^2 + \epsilon_0(\nabla^2 - \partial^2/\partial y^2) & j\epsilon_d\nabla_\perp^2 + \epsilon_0(\partial/\partial x\partial y) & \epsilon_s(\partial^2/\partial x\partial z) + j\epsilon_d(\partial^2/\partial y\partial z) \\ -j\epsilon_d\nabla_\perp^2 + \epsilon_0(\partial^2/\partial x\partial y) & \epsilon_s\nabla_\perp^2 + \epsilon_0(\nabla^2 - \partial^2/\partial x^2) & \epsilon_s(\partial^2/\partial y\partial z) - j\epsilon_d(\partial^2/\partial x\partial z) \\ \epsilon_s(\partial^2/\partial x\partial z) - j\epsilon_d(\partial^2/\partial y\partial z) & \epsilon_s(\partial^2/\partial y\partial z) + j\epsilon_d(\partial^2/\partial x\partial z) & \epsilon_s(\nabla^2 + \partial^2/\partial z^2) \end{bmatrix} \tag{4}$$

$$\hat{E} = \begin{bmatrix} \epsilon_0\epsilon_s & j\epsilon_0\epsilon_d & 0 \\ -j\epsilon_0\epsilon_d & \epsilon_0\epsilon_s & 0 \\ 0 & 0 & \epsilon_{+1}\epsilon_{-1} \end{bmatrix}$$

Case B

For wave frequencies in the range $\frac{1}{2}\omega_{He} > \omega > \omega_{LHR}$, there exist three distinct stationary points: $\theta_1 = 0$, and $\theta_{2,3} = \pm\cos^{-1}(2\epsilon_s/\epsilon_d)$, two of which lie within the range of integration of (5). For this case, $I(\boldsymbol{R})$ has the form

$$I_B(\tilde{z}) \cong I_A(\tilde{z}) - |\pi/k_0\lambda|^{3/2} \frac{(-a)^{1/4}\exp j(2k_0\lambda\sqrt{-a}\,|\tilde{z}| - \pi/4)}{2\epsilon_0\epsilon_d|\tilde{z}|^{1/2}},$$
$$a = \epsilon_{+1}\epsilon_{-1}/\epsilon_s. \qquad (8)$$

Case C

When $\omega = \omega_{He}/2$, the three stationary points mentioned above merge to form a third-order stationary point at $\theta = 0$. Here $I(\boldsymbol{R})$ has the form

$$I_C(\tilde{z}) \cong -\sqrt{2}\left(\frac{\pi}{k_0}\right)^{3/2} \frac{\epsilon_{+1}^{1/4}\exp - j(k_0\sqrt{\epsilon_{+1}}\,|\tilde{z}| + \pi/4)}{\epsilon_0\epsilon_d|\tilde{z}|^{1/2}}. \qquad (9)$$

Note that for $\lambda = -0.5(-a \to \epsilon_{+1})$, neglecting the higher order term of $I_A(\tilde{z})$, $I_B(\tilde{z})$ reduces identically to $I_C(\tilde{z})$, as it should.

Case D

When $\omega \to \omega_{LHR}$, the dimensions of the source become important and, in general, the assumption that $k_0\mu(\theta)\tilde{\rho} < 1$ for all source points becomes untenable. In this case, the approximation of $I(\tilde{R})$ can proceed along lines explored previously by others [3]–[6], and we do not give this result here.

Substituting (7), (8), and (9) into (2), the explicit form of the tensor Green's function $G(\boldsymbol{r} - \boldsymbol{r}')$ can be found for the three cases discussed above:

$$\hat{G}_A \cong \frac{-jk_0Z_0\exp(-jk_0\sqrt{\epsilon_{+1}}\,|\tilde{z}|)}{2\pi(1+\lambda)(1+2\lambda)|\tilde{z}|}\hat{A} \qquad (10)$$

$$\hat{G}_B \cong -|k_0\lambda\pi|^{3/2}\frac{\pi Z_0(-a)^{1/4}\exp j(2k_0\lambda\sqrt{-a}\,|\tilde{z}| - \pi/4)}{8|\tilde{z}|^{1/2}}\hat{B} \qquad (11)$$

$$\hat{G}_C \sim -\left(\frac{k_0}{2\pi}\right)^{1/2}\frac{k_0Z_0\epsilon_{+1}^{1/4}\exp - j(k_0\sqrt{\epsilon_{+1}}\,|\tilde{z}| + \pi/4)}{2|\tilde{z}|^{1/2}}\hat{A} \qquad (12)$$

where the nonvanishing matrix elements of $\hat{A}$ and $\hat{B}$ are

$$A_{11} = A_{22} = 1$$
$$A_{12} = -A_{21} = j$$
$$B_{11} = B_{22} = (\epsilon_s + a)/\epsilon_d$$
$$B_{12} = -B_{21} = j$$
$$B_{33} = [16\lambda^4a^2 + \epsilon_{-1}\epsilon_{-1}(1 + 8\lambda^2)]/\epsilon_0\epsilon_d$$

and

$$Z_0 \simeq \sqrt{\mu_0/\epsilon} \cong 377 \text{ ohms}.$$

III. Applications

In applying the tensor Green's function developed in Section II, we consider the power flux along the static magnetic field for an infinitesimal electric dipole of moment I_0h (approximating a small dipole with a triangular current distribution) and a filamentary loop of radius h, with either parallel or perpendicular orientation with respect to the magnetic field. The calculation will be made only for the case of $\omega = \omega_{He}/2$, a frequency at which VLF emissions are often observed.

A. Perpendicular Dipole

$J(r')$ is given by $I_0h\delta(\boldsymbol{r}')\boldsymbol{a}_x$. Using (1) and (12), the Cartesian components of the electric fields are found at $\tilde{\rho} = 0$ (along z axis):

$$E_x \simeq -\left(\frac{k_0}{2\pi}\right)^{1/2}\frac{(I_0hk_0)Z_0\epsilon_{+1}^{1/4}}{2|z|^{1/2}}\exp - j(k_0\sqrt{\epsilon_{+1}}\,|z| + \pi/4)$$
$$E_y = -jE_x$$
$$E_z = 0. \qquad (13)$$

Using (13) along with the relations $\boldsymbol{H} = j\nabla \times \boldsymbol{E}/\omega\mu_0$ and $S = \operatorname{Re}\boldsymbol{E} \times \boldsymbol{H}^*/2$, the Poynting flux along z axis can be determined:

$$S_z \simeq \frac{(I_0hk_0)^2Z_0}{4\pi}\frac{\omega_p}{\omega_{He}}\frac{k_p}{z} \qquad (14)$$

where ω_p is the plasma frequency and $k_p = \omega_p/c$.

From $G_{11} = G_{22}$ (the first two diagonal components of $\hat{G}$), it is clear that for the same dipole oriented along y axis, P_z again is given by (14).

B. Parallel Dipole

For this case, $J(r')$ is given by $I_0h\delta(\boldsymbol{r}')\boldsymbol{a}_z$ and since $A_{13} = A_{23} = 0$, there is no transverse component of the electric field at the z axis. Therefore, $P_z = 0$ for all three frequency ranges considered in the previous sections. This result is a special case of a general rule that can be inferred from symmetry arguments, that is, any source symmetric about the z axis cannot produce a nonvanishing component of E_x or E_y at the z axis. Thus a loop antenna with its symmetry axis parallel to the field line and no azimuthal variation of current will also yield zero Poynting flux exactly along the field.

C. Two Dipoles with Circular Phasing

For this case, we consider two dipoles oriented along the x,y axis and 90° out of temporal phase. $J(r)$ is then expressed by

$$J(r) = I_0h(\boldsymbol{a}_x \pm j\boldsymbol{a}_y)\delta(\boldsymbol{r}) \qquad (15)$$

with + and − being, respectively, the left and right circular polarization. Using (1), (12), and (15), the electric field can be calculated:

$$E_x \simeq -\left(\frac{k_0}{2\pi}\right)^{1/2}\frac{I_0hk_0Z_0\epsilon_{+1}^{1/2}}{|z|^{1/2}}\begin{pmatrix}0\\1\end{pmatrix}\exp - j(k_0\sqrt{\epsilon_{+1}}\,|z| - \pi/4)$$
$$E_y = -jE_x. \qquad (16)$$

For these field components, the Poynting flux becomes

$$S_z \simeq \frac{(I_0hk_0)^2Z_0}{\pi}\frac{\omega_p}{\omega_{He}}\begin{pmatrix}0\\1\end{pmatrix}\frac{k_p}{z}. \qquad (17)$$

In (16) and (17), the upper and lower elements of [illegible] correspond to the $\pm$ sign of (15), respectively.

D. Perpendicular Loop

For this case, we orient the loop (of radius h) in the x-z plane, with its axis of symmetry along y axis. The current $J(r)$ in spherical coordinates can be written

$$J(r) = \frac{I_0\delta(r - h)}{h\sin\theta}[\delta(\phi - \pi) - \delta(\varphi)]\boldsymbol{\theta} \qquad (18)$$

where $\boldsymbol{\theta}$ is a unit vector in the direction of increasing θ. Using (18), (1), and (12), the transverse components of $\boldsymbol{E}$ can be found:

$$E_x \simeq \frac{j(k_0\pi)^{3/2}I_0(hk_0)^2Z_0\epsilon_{+1}^{3/4}}{\sqrt{2}|z|^{1/2}}\exp(-j\sqrt{\epsilon_{-1}}k_0|z|)$$
$$E_z = 0 \quad ; \; E_y = -jE_x \qquad (19)$$

with the resulting Poynting flux

$$S_z \cong 2\pi^3I_0^2(hk_0)^4Z_0(\omega_p/\omega_{He})^3(k_p/z). \qquad (20)$$

From the above results, it is interesting to note the following:

1) From (14), (17), and (20), it is seen that the focusing effect along the field line, as $z \to \infty$, is proportional to the first power of the effective distance k_pz measured by the plasma wavelength in the medium.

2) Comparing (17) with (14), it is concluded that, at $\omega = \omega_{He}/2$, a right-handed circularly polarized dipole can radiate four times as much longitudinal power as a single dipole, while a left-handed circularly polarized dipole cannot radiate energy exactly along the field line.

3) A perpendicular loop with a diameter equal to the length of the dipole can radiate $\frac{1}{2}\pi^4(hk_p)^2$ times the power of the single dipole. Thus depending upon the plasma density, the loop can either radiate more or less energy along the field line than a dipole.

IV. Discussion

From the explicit forms of the tensor Green's function given in Section II, it is clear that focusing effects along the field line take place only for frequencies in the range $\omega_{LHR} < \omega \leq \omega_{He}/2$. Within this range, the fields vary with distance $z^{-1/2}$ instead of varying customarily as z^{-1}, and the focusing effect is such that the relative enhancement of wave energy along the field line direction is proportional to the first power of the distance in the far zone.

A somewhat more quantitative estimate of the relative enhancement of wave energy along the field line direction can be obtained by noting in (5) that as the observation point moves away from the z axis, the large argument approximation of the Bessel function, i.e., $J_0(x) \sim \sqrt{2/\pi x} \cos(x - \pi/4)$, must eventually be used in conjunction with a saddle-point approximation of the integral. In this regime, the new tensor Green's function $\hat{G}_B'$ will have the approximate value $\hat{G}_B' \approx [k_0\mu(\theta_s)\tilde{\rho}]^{-1/2}\hat{G}_B$, where θ_s is the value of θ at the saddle point defined by the relation $\rho d\mu/d\theta = z d\nu/d\theta$, and the wave energy should drop off approximately as $[k_0\mu(\theta_s)\rho]^{-1}$ as the observation point moves out sufficiently far from the z axis. Since the quantity $k_0\mu(\theta_s)$ is generally of the order 10 km^{-1} for VLF waves in the magnetosphere, it is evident that the drop-off in wave energy from the lobe maximum can be rapid and that consequently the longitudinal focusing of VLF waves can be important as a means of obtaining enhanced wave amplitudes from a low-power satellite transmitter.

The work of previous authors [3]–[6] has made it clear that focusing effects in a cold magnetoplasma may also occur for ray directions which are inclined to the static magnetic field line direction, and thus the far-field radiation pattern from a given source may possess not only a major lobe along the magnetic field line direction, but also one which is inclined at some finite angle to this direction.

This nonlongitudinal focusing takes place as a result of the presence of inflection points in the refractive index surface, and as a result of this focusing the far fields drops off like $r^{-5/6}$ [3] and the radiation flux drops off like $r^{-5/3}$. Since the longitudinally focused energy flux, as shown above, drops off like r^{-1}, it is clear that in theory the longitudinal lobe must predominate as $r \to \infty$. Whether or not the longitudinal lobe will predominate in an experimental situation will depend upon the scale of homogeneity of the magnetospheric plasma as well as upon the details of the radiating source function. Further study of these effects is now in progress and results will be presented in a future paper.

T. N. C. Wang
T. F. Bell
Radioscience Lab.
Stanford University
Stanford, Calif.

References

[1] "Physics of the earth in space," Space Science Board, Woods Hole, Mass., NAS/NCR Tech. Rept., August 1968.
[2] R. A. Helliwell, J. Katsufrakis, M. Trimpi, and N. Brice, "Artificially stimulated very-low-frequency radiation from the ionosphere," *J. Geophys. Res.*, vol. 69, pp. 2391–2394, June 1964.
[3] E. Arbel and L. B. Felsen, "Theory of radiation from sources in an anisotropic media, part II," in *Symp. on Electromagnetic Theory and Antennas*, pt. I. E. C. Jordan, Ed. New York: Pergamon, 1963, pp. 421–459.
[4] F. V. Bunkin, "On radiation in anisotropic media," *J. Exptl. Theorit. Phys.* (USSR), vol. 32, pp. 338–346, 1957.
[5] H. H. Kuehl, "Electromagnetic radiation from an electric dipole in a cold anisotropic plasma," *Phys. Fluids*, vol. 5, pp. 1095–1103, 1962.
[6] H. Kogelnik, "On electromagnetic radiation in magnetoionic media," *J. Res. NBS*, sec. D (Radio Propagation), vol. 64, pp. 515–523, 1960.
[7] J. A. Ratcliffe, *The Magneto-Ionic Theory and Its Applications to the Ionosphere.* New York: Cambridge, 1959.
[8] W. S. Ament, M. Katzin, J. R. McLaughlin, and W. W. Zachary, "Satellite antenna radiation properties at VLF in the ionosphere," Electromagnetic Research Corp., College Park, Md., Rept. ONR-4250-1, 1965.
[9] T. N. C. Wang and T. F. Bell, "On radiation resistance of a 'short' dipole in a cold magnetoionic medium," *Radio Sci.*, vol. 4, pp. 167–177, February 1969.

Transionospheric Radio-Ray-Path Rate of Change from Polarization and Frequency Measurements of Satellite VHF Signals

***Abstract*—The rate of change of the radio-ray-path length for transionospheric satellite signals is determined from Doppler and Faraday effect analyses for quiet ionospheric conditions. VHF beacon signals are used. The transionospheric path length of 40-MHz signals showed a natural oscillatory behavior of 1 wavelength per second.**

Determination of a natural rate of change of the actual ray-path length of a signal traversing ionospheric regions is important, for example, in VHF radio-location and direction-finding problems. The ray-path length difference between two positions of the satellite and the ground station defines the total rate of change of the ray path. When the ionosphere is assumed to vary, the effects from the medium's rate of change as well as those from satellite motion will be reflected in the total rate of change of the ray path. Effects from the medium are reduced when ionospheric conditions are stable and can be assumed to display neither frequency [1] nor polarization [2] scintillations. Our determination of the ray-path rate of change for such quiet conditions utilizes an analysis of the 40-, 41-, and 360-MHz beacon signals of satellite S-66 BEC. Faraday rotation and Doppler shift data are taken every second. Variations between a smoothed fit to the data and the actual data reflect the variations caused by the medium.

The equation defining the Doppler shift in the ionosphere using only first-order approximation for the refractive index is

$$\Delta f = (f/c)\dot{S} - (k/cf)\dot{n}_t \tag{1}$$

where f is the frequency, c the speed of light in vacuum, $\dot{S}$ the rate of change of the radio ray path, $k = 4.03 \times 10^7$ in cgs units, and n_t the integrated electron density N_e along the radio ray path:

$$n_t = \int_0^S N_e \, ds.$$

The equation defining the Faraday rotation in the ionosphere (again with first-order approximation for the index of refraction) is

$$a = (K/f^2)\mathbf{M}n_t \tag{2}$$

where a is the polarization rotation angle, $\mathbf{M}$ the effective geomagnetic field component at ionospheric heights, and K a constant equal to 2.36×10^4 (cgs units). Combining (1) with differentiated (2) we obtain

$$\dot{S} = \frac{c}{f}\Delta f + \frac{k}{K}\left[\frac{\dot{a}}{\mathbf{M}} - \frac{\dot{\mathbf{M}}a}{\mathbf{M}^2}\right]. \tag{3}$$

Taking the variation of both sides of (3), we obtain

$$\delta\dot{S} = \frac{c}{f}\delta(\Delta f) + \frac{k}{K}\delta\left[\frac{\dot{a}}{\mathbf{M}} - \frac{\dot{\mathbf{M}}}{\mathbf{M}^2}a\right]. \tag{4}$$

The following interpretation is then used in considering that the left-hand side of (4) represents the momentary deviation of the path length's rate of change in comparison to a smoothed variation. The first term on the right represents the path change according to the measured frequency scintillations [1], whereas the second term is derived from polarization measurements [see (2)]. The term $\delta(\Delta f)$ is the measured momentary deviation of the observed frequency from a fitted curve through all observed frequency points; similarly, $\delta[\dot{a}/\mathbf{M} - \dot{\mathbf{M}}/\mathbf{M}^2]$ represents the momentary deviation of the observed values from the corresponding value of a best-fitting curve through all observed values of a and $\dot{a}$. The two terms in (4) are determined by the medium. Instabilities of the ionospheric electron content have a strong effect upon Δf from both terms in (1); small

Manuscript received May 1, 1969.